ACOUSTIC WAVE INTERFEROMETERS

Propagation of sound in a medium is a wave phenomenon and thus exhibits interference. In fact, interference is observed when two coherent waves are allowed to be superimposed in space. It is possible to obtain two coherent waves by splitting a single wave either at its wavefront, by passing through two or more apertures, or in its amplitude, by reflection and transmission at the interface of media of different phase velocity and/or density. The interference pattern at any point depends on the phase difference (relative time delay) caused by the propagation of these initially coherent waves through different acoustic paths.

When two sound waves interact with a particle of the propagation medium, the resultant displacement, velocity, and pressure are the vector sum of the effects due to the separate waves. If the final distribution of energy for this particle is different from what it would have been for each separate wave, interference has occurred. This phenomenon may be used to determine the relative physical properties of the media through which these waves have traveled prior to their superimposition. If two or more coherent waves propagate along a different acoustic path with respect to the reference material or to each other, their superimposition produces fringes (i.e., alternating regions of constructive and destructive interference, with a maximum or minimum of intensity, respectively). The shape of these regions depends on the geometry of the media causing the path difference. Thus a properly designed acoustic interferometer (or an interferometer, in general) behaves as a differential device since it transforms the phase difference of the initially coherent wave into intensity modulation.

A variety of experimental acoustic (and ultrasonic) techniques for material characterization have been developed in recent decades: for example, time-of-flight methods, photoelastic and acoustoelastic techniques, pulse-echo overlap methods, and phase detection methods (1). Among all these techniques, the interferometric ones, based on the aforementioned phenomenon of interference, present several advantages as far as accuracy and reproducibility of the measurements are concerned. In fact, they are not based on the measurement of absolute values, like other techniques, but rather on the determination of differences between reference signals and perturbed ones (e.g., phase shifts, frequency shifts) (2). Such differences are responsible for destructive or constructive interference between signals, which can be measured with high precision by using simple experimental setups. Other advantages of acoustic interferometry are as follows:

1. Its applicability to very small samples
2. Its ability to measure simultaneously both velocity and attenuation
3. The possibility of using noncontact detectors
4. The higher precision that may be obtained from the direct measurement of the difference between unperturbed and perturbed quantities

A proper logical control device is connected to the detector in order to trigger, both in amplitude and frequency, the signal generator of the acoustic wave until a specific interferometric pattern is achieved. This capability is exploited when the interferometric device is used to measure the triggering required for reproducing the same pattern under different external conditions. In this case the precision and sensitivity of the instrument can be highly enhanced.

Although all interferometers are based on the same simple general principle, several different realizations may be designed. First, acoustic waves may interfere directly or can be used to produce an electric signal or to modify the path of an optical wave, and then be used for interference. Second, different techniques may be used for generating the path difference. The simplest way is to let the wave experience multiple reflections at the interfaces of the propagation medium. Alternatively, the input and output signals may be correlated or two different input signals injected in different locations may be used.

Acoustic interferometers are used both for measuring the actual phase velocity and attenuation factor of the propagation medium and for evaluating their variation in the presence of a perturbation (e.g., pressure variation, presence of impurities) with respect to a reference case (ambient pressure, homogeneous specimen, etc.). In the first case, the physical properties are directly correlated to the position and intensity of the maxima and minima of the interference pattern. In the second case, higher accuracy may be obtained if some device characteristics (e.g., position, frequency) are properly modified in order to reproduce the same interference pattern as in the unperturbed case (in particular, the conditions for destructive interference).

To obtain constructive and/or destructive interference fringes, the acoustic path difference between the two interfering beams must be at least one-half of a wavelength. This puts constraints on the specimen thickness (or allowed variation of it) and the frequency of the acoustic wave employed. For low frequencies, one may need a thicker specimen in order to obtain several fringes, whereas for higher frequencies the required variation in an acoustic path may be smaller, provided that the attenuation is low enough to have a signal-to-noise ratio greater than one.

Acoustic interferometric techniques may be realized by means of a proper experimental setup or a specific interferometric device. In the next section, we discuss the first case, in which interference of acoustic waves is realized and the interference pattern is directly sensed by a transducer. The following section is devoted to the description of indirect interferometric techniques, which analyze the interference in an electronic device (e.g., an oscilloscope) between the electric signal feeding the transducer and the one induced by the acoustic wave at the receiver. Then the operational principles of quadrature detector systems, which may be used to improve the performance of interferometers, are briefly described. Since in recent years great effort has been devoted to developing techniques based on optical sensors and interferometers, in the last section a brief comparison is made between acoustic and other interferometric techniques.

DIRECT ACOUSTIC INTERFEROMETRIC TECHNIQUES

In direct interferometric techniques the interference occurs among acoustic waves and the interference pattern is sensed by a transducer. One of the earliest demonstrations of acous-

J. Webster (ed.), *Wiley Encyclopedia of Electrical and Electronics Engineering.*

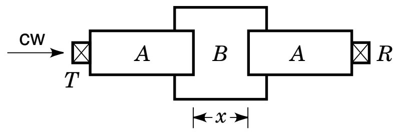

Figure 1. Scheme of a standing wave acoustic interferometer for the determination of the acoustic properties of the material B.

tic interference was carried out by Quincke in 1866 (3) by using an apparatus suggested by J. Herschel. It consisted of a tube, which branched into two tubes differing in length by an odd number of half wavelengths of sound in air and joining again at the other end into a single tube. Stewart (3) modified this interferometer by using equal-length branches but varying the frequency in order to obtain interference. A more sophisticated tool for measuring the velocity in gases consisted of a column formed by an ultrasonic transducer and an adjustable reflecting piston (4).

In more recent times, a simple setup, called a standing wave acoustic interferometer, has been used for the characterization of molten materials, such as metals or alloys, and dense fluids (5,6). A continuous wave (cw) is injected from the left side of a sandwich, composed of two external layers (A) of known properties and an intermediate layer (B) of the molten or fluid material, whose acoustic properties need to be determined (Fig. 1). The output signal is detected by a receiver (R) at the right side of the setup. The impedance mismatch at the interfaces between the materials A and B generates multiple reflections that interfere with each other. A resonant constructive standing wave is formed when the thickness x of the layer B is equal to integer multiples of half wavelengths, while antiresonant conditions occur when

$$x = (n + 1/2)\frac{\lambda}{2} \tag{1}$$

By varying the thickness x (and the geometry) of B, the transmitted ultrasonic signal traces out an interference pattern with alternating maxima and minima (Fig. 2). By fitting the curve amplitude versus thickness, according to simple theoretical expressions, the phase velocity and attenuation factor may be easily calculated.

A particularly suitable setup consists of two movable metal rods partially submerged in a tank containing the molten material. Thus the thickness of B can be easily varied with continuity. In this case, the analytical expression for the wave amplitude at the receiver is given by (5)

$$\frac{1}{|A|} = \frac{1}{4}\sqrt{\begin{aligned}&2(4+H)\cosh\left(\frac{\beta x}{Q}\right) + 8F\sinh\left(\frac{\beta x}{Q}\right)\\ &\quad +2(4-H)\cos(2\beta x) - 8G\sin(2\beta x)\end{aligned}} \tag{2}$$

where F, G, and H are functions of the acoustic impedances of the rod and the molten material and β and Q are the real part of the wave number in the molten material and the quality factor, respectively. Both may be evaluated through a least-squares fitting of the experimental data (Fig. 2) with Eq. (2). Thus, the same measurement allows one to compute the phase velocity v_B and the specific attenuation factor α for the medium B:

$$v_B = \frac{\omega}{\beta}; \quad \alpha = \frac{\beta}{2Q} \tag{3}$$

where ω is the known carrier-wave frequency.

Several effects may affect the accuracy of the standing wave acoustic interferometric technique (e.g., beam spreading in layer B or lack of parallelism and flatness of the A faces). However, the technique is rather accurate as far as the measurement of the velocity is concerned.

A similar approach has been used (7) for determining the speed of sound in gases by evaluating the resonant frequencies in a cylindrical interferometer. A transducer is used for generating an acoustic wave in a gas inside an acoustical cavity. Longitudinal modes are formed, due to interference between multiple reflecting waves, with resonance frequencies

$$f_n = \frac{u}{2L}(n + \delta) \tag{4}$$

where L is the length of the cavity, u the sound speed, n the order of the resonance, and δ a phase shift correction due to the finite diameter of the cavity. The resonant frequencies are measured through an oscilloscope, and a fitting with Eq. (4) yields optimal values for the parameters u and δ.

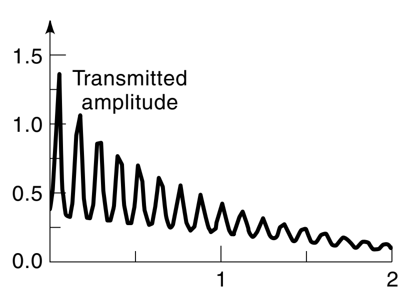

Figure 2. Interference pattern obtained with the standing wave acoustic interferometer.

INDIRECT ACOUSTIC INTERFEROMETRIC TECHNIQUES

In indirect acoustic interferometric techniques the interference occurs between the electric signal feeding the transducer and the one induced by the acoustic wave at the receiver. The simplified circuit diagram (neglecting almost all electronic components) of a typical interferometric device (8) is reported in Fig. 3. A generator feeds a signal into a doubler (not reported in Fig. 3), which splits the signal into two components, called reference and testing signals. The latter is amplified by a power amplifier and converted into an ultrasonic pulse by a piezoelectric (or other) transducer. The signal detected by the receiver passes through a low-noise amplifier and is recombined in the region H with the unperturbed reference signal, thus producing interference. In Fig. 3(b), a zooming of the region H is reported for a two-channel quadrature detection system (described later) (9). Before interference the reference signal is split in A into two arms in quadrature. Then each one is combined in C with the testing signal split in B into two arms in phase. The two channels are usually named cosine and sine channels.

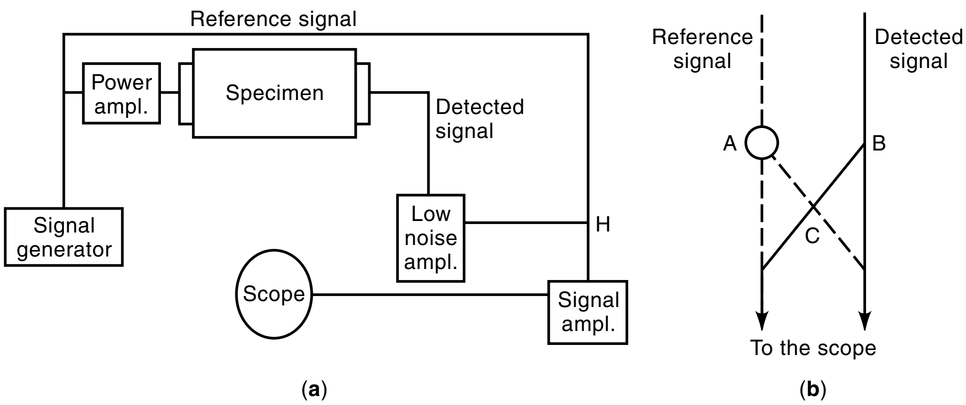

Figure 3. (a) Simplified circuit diagram for an indirect acoustic interferometric setup. (b) Scheme of the quadrature detection system.

This technique is particularly efficient for evaluating the variations of a physical parameter of the specimen due to external perturbations. For such a purpose, the frequency of the reference signal is modulated in order to maintain quadrature (i.e., a destructive interference) when the intensity of the perturbation is changed. The fractional change in the interferometer frequency with respect to the nonperturbed case gives, through simple relationships, the variation of the physical parameter.

To clarify the method, we discuss its use (10) for the determination of the acoustic nonlinearity parameter B/A, defined as

$$\frac{B}{A} = 2\rho_0 c_0 \frac{\Delta c}{\Delta p} \tag{5}$$

where ρ_0 is the medium density, c_0 the sound velocity, and Δc the velocity variation resulting from a pressure change Δp for an isoentropic transformation. A sample material maintained at a constant temperature is pressurized with different values of p. For each pressure, the effective path length between the transducers changes due to a variation of the sound velocity in the propagation medium. An adjustment of the transmitted frequency is necessary in order to maintain quadrature. Then the parameter B/A can be easily evaluated from the fractional change in the interferometer frequency $\Delta f/f_0$ necessary to maintain quadrature:

$$\frac{B}{A} = 2\rho_0 c_0^2 \frac{\Delta f}{f_0\,\Delta p} \tag{6}$$

where f_0 is the reference frequency. In this situation the velocity variation is measured with a very high accuracy (up to 1%).

A similar approach is based on the measurement of the crosscorrelation function between the signals from the receiver (R) and the transmitter (T) (8,11–19). For example (11,12), continuous waves of suitable frequency (1 MHz to 20 MHz) are split into two parts. One portion of these waves excites an immersion transducer, while the other (reference signal) is fed into a phase-sensitive detector. The specimen is submerged in water and oriented in such a way that the incident beam scans its surface at a fixed angle. Receiver and transmitter are mounted on the same bridge and initially located and oriented so that the received signal (testing signal) is maximum. The amplitude of the signal resulting from the crosscorrelation between the reference and testing signals is measured for different positions of the transducer. It depends, of course, on the length of the effective acoustical path of the testing wave from T to R, leading to plots similar to the one reported in Fig. 2.

When the geometry of the specimen is properly defined, this crosscorrelation technique leads to results that can be easily interpreted in terms of the relevant physical variables. A particularly interesting case occurs when the material specimen is cut in the shape of a wedge (11) (Fig. 4). In fact, if the material is homogeneous, the only difference between waves entering the wedge at different locations (e.g., T and T' in Fig. 4) is their length y of propagation path within the material, since all other factors, such as boundary conditions, remain identical. Therefore, the results depend only on the interference effects and are not affected by the angular dependence of reflection, refraction, and mode conversion, which in general greatly complicate the physical picture.

Assuming that the wedge angle is small, the ultrasonic signal S_T, sent by the transmitter, and S_R, received by the transducer R, are given by

$$\begin{aligned} S_T &= F_T A_0 \cos(\omega t + \Phi_0) \\ S_R &= T_{12} T_{21} F_R A_0 \exp[-\alpha_1 (l-y) - \alpha_2 y] \\ &\quad \cos\left(\omega\left\{t - \left[\frac{l-y}{v_1}\right] - \frac{y}{v_2}\right\} + \Phi_0\right) \end{aligned} \tag{7}$$

where F_T and F_R are the response factors of the transmitter and of the receiver and associated electronics; T_{12} and T_{21} are the transmission factors between water and the specimen material and vice versa; α_1, α_2, v_1, and v_2 are the attenuation coefficients and phase velocities in water and in the material,

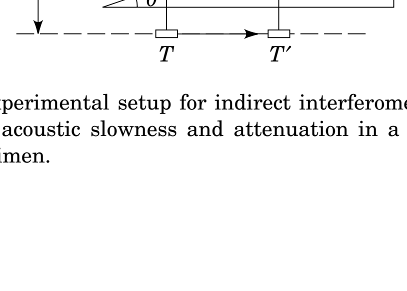

Figure 4. Experimental setup for indirect interferometric measurements of the acoustic slowness and attenuation in a wedge-shaped material specimen.

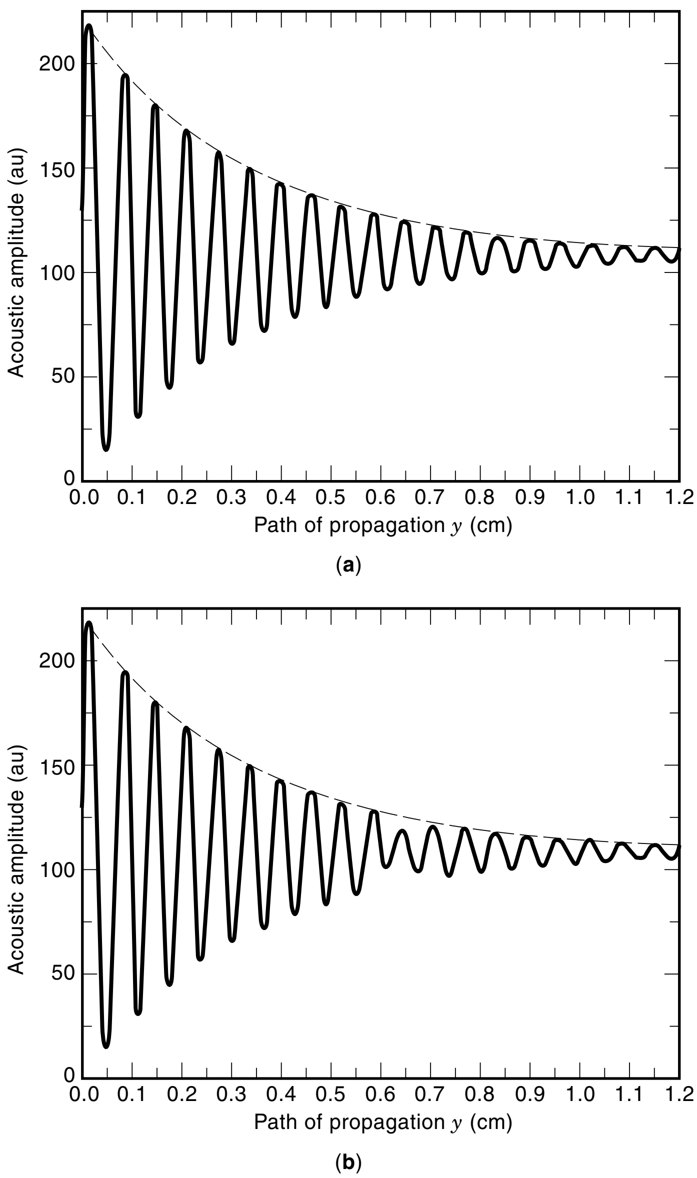

Figure 5. Typical experimental crosscorrelation curves obtained using the wedge-shaped specimen shown in Fig. 4. (a) Specimen without defects. (b) Specimen with a hole drilled into it. The frequency is in both cases $f = 11$ MHz.

respectively; A_0 is the initial amplitude of the cw; and l is the fixed distance between the transducers T and R.

After some algebraic manipulation, one finds that the crosscorrelation factor between the two signals S_T and S_R is given by (11)

$$\Psi = \Psi_0 + C \exp(-\alpha y) \cos(by + \Phi) \tag{8}$$

where Ψ_0, C, α, b and Φ are parameters that can be found by least-squares fitting the experimental curves (see, e.g., Fig. 5a). Since

$$\alpha = \alpha_2 - \alpha_1 \tag{9}$$

$$\beta = \omega \left(\frac{1}{v_2} - \frac{1}{v_1} \right) \tag{10}$$

one immediately obtains the attenuation coefficient and phase velocity for the material, since the values of the corresponding quantities for water are well known. It is worthwhile to remark that Fig. 5(a) yields α_2 and v_2 by simple inspection, since α_2 is given by the coefficient of the envelope curve $\exp(-\alpha y)$ and v_2 by the distance between successive maxima and minima.

This technique may also be used for the detection of flaws in the material specimen. In fact, in the presence of defects the crosscorrelation plot is locally modified [see Fig. 5(b)] and from the difference between the two plots (the so-called signature of the defect) the main features of the flaw may be evaluated.

Since for practical purposes material plates are much more important than wedges, the method has been extended to the treatment of plates (12). The main ingredient (i.e., the continuous variation of the acoustic path in the material specimen y) is obtained by slowly varying the angle of incidence. Also in this case it is possible to obtain the attenuation coefficient and phase velocity of the material through a best fitting of the theoretical formula. The fitting formulas are, however, more complicated and the measured attenuation is no longer absolute, since there are boundary effects depending on the incidence angle.

QUADRATURE DETECTOR SYSTEMS

A quadrature detector system is an interferometer based on comparison between the correlations of the testing signal with two reference signals in quadrature in two different channels (cosine and sine channels). To illustrate the operation of an ideal quadrature detector system (see Fig. 3), let us consider a wave train of angular frequency ω and wavelength λ crossing a path length L in a medium with propagation velocity c. If $w = \cos(\omega t)$ is the transmitted signal, the received signal is in the form

$$s = A \cos \left(\omega t - \frac{2\pi L}{\lambda} \right) \tag{11}$$

where A is its amplitude. The testing signal is then demodulated in the two channels of the quadrature detector with two reference signals $u = 2 \cos(\omega t)$ and $v = -2 \sin(\omega t)$. Neglecting high-frequency contributions (filtered out by a low-pass filter), the two detected signals are $u_1 = A \cos(2\pi L/\lambda)$ and $u_2 = A \sin(2\pi L/\lambda)$. The pair ($u_1$, u_2) are components of a vector $\mathbf{u}$ with constant modulus, which rotates when L varies. The number of fringes η crossed by the vector $\mathbf{u}$ can be easily counted by recording the zeroes of u_1 and u_2. The change in path length is then given by

$$\Delta L = (\eta + F) \frac{\lambda}{4} \tag{12}$$

where F is the fractional number of fringes, obtained by interpolation between the counts.

All interferometers with quadrature detector systems are affected by a set of errors (9), which in many cases severely limit the precision and accuracy of the measurements. These errors are due to a lack of quadrature between the reference signals (the phase shift is not exactly $\lambda/4$), to an unequal gain in the detector channels, and to an error in the zero offsets of the device. Moreover, in real systems, due to electronic and mechanical overtones (nonlinearity), higher-harmonics effects are always present and will severely affect the evaluation of transient times. Therefore, while for an ideal quadrature detector system the precision is limited only by the system noise, in real cases the endpoint of the vector **u**, is no longer on a circle and F is affected by an error, causing errors in ΔL up to a few percent of λ, which is very large compared to the accuracy of a good interferometer. If r is the channel gain ratio, p and q are the offsets in the cosine and sine channels, and α is the reference signal quadrature error, the output signal from the detector becomes

$$u_1^D = u_1 + p \tag{13}$$

$$u_2^D = \frac{1}{r}(u_2 \cos\alpha - u_1 \sin\alpha) + q \tag{14}$$

describing an ellipse. The real signals can, however, be easily reconstructed from the ones used in Eqs. (13) and (14), since we are considering systematic errors and therefore the corrections p, q, r, and α must be calculated only once. By several measurements of u_1^D and u_2^D for a few sets of known values of ΔL, the parameters p, q, r, and α can be obtained by least-squares fitting the distorted ellipse equation to the experimental data. Such an approach allows one to reach a resolution on the order of 10^{-8} m, 100 times higher than the one obtained with uncorrected data.

By using a similar approach, it is possible to introduce corrections taking into account the transformation of the ellipse into a deformed ellipse due to the presence of higher-order harmonics. Such corrections are obtained by using the least-squares method iteratively (20).

OTHER INTERFEROMETRIC TECHNIQUES

There are many other types of devices, e.g., acoustic spectrometers (21) and acoustic microscopes (22) which use the underlying principles of interferometry for their operation but have not been labeled as interferometers. Acoustic spectrometers are used to measure frequencies of mechanical resonances (standing waves in the thickness of the specimen) caused by interference between the normal incident acoustic waves and the ones reflected from the back surface of a parallel plate. These resonances are obtained by varying the frequency of the incident plane wave or by varying the thickness (e.g., corroded steel plates) for a broadband incident pulse. The resonant frequencies and Q-factor of these resonances are used to compute phase velocity and attenuation. Both of these quantities can be used to characterize the material.

The acoustic microscope is also an example of a device based on interference phenomena. It can be designed for various applications to materials and tissue characterization. For example, a specially designed acoustic lens (with aperture angle larger than Rayleigh critical angle) facilitates the oscillations in a quantity $V(z)$ which is the record of the modulus of the measured voltage as a function of the z distance between the focal point of the acoustic lens and the specimen surface. These oscillations are due to interference between the normal specular reflection from the fluid-loaded surface of a solid specimen and a ray passing through the Rayleigh critical angle. The velocities and attenuation of elastic wave propagation mode can be obtained from the periodicity and decay of $V(z)$. Theoretical fit of the velocities with those obtained from $V(z)$ determines elastic constants which are useful for characterization of thin films deposited on an elastic substrate (see Achenbach et al., Ref. 23).

Different types of interferometers based on optics have also been developed (e.g., the Mach interferometer) for the purpose of detecting the gas flow in supersonic wind tunnels. Displacements of the interference fringes in the optical wavefront, traveling normal to the gas flow and the reference beam, can be used to determine the density change in the gas flow. A coupling of the light beam to the specimen (gas flow) does not perturb its initial phase. Conversely, ultrasonic nondestructive evaluation may require the use of contact transducers, which perturb the system and therefore the accuracy of specific measurements. For instance, wave attenuation measurements are severely limited by the mode conversion of the wave at the interface between the medium and the transducer. In fact, such an effect becomes, in many cases, the dominant contribution to the measured attenuation factor. To overcome this difficulty, considerable effort has been devoted to the development of optical techniques for the generation and detection of ultrasonic waves. Such techniques are based on the so-called photoacoustic effect; for example, the generation of an ultrasonic pulse through a laser beam incident on an elastic specimen (24) and the evaluation of the acoustic wave amplitudes through modulations of the optical phase of a light beam (25–31). In the latter, the phase shift may be demodulated to a change in optical intensity through an optical fiber interferometer. The acoustic wave amplitude and/or the acoustic properties of the medium can be easily obtained from these measurements. Optical methods are particularly suitable for determination of the dispersion law of the medium, since optical interferometers measure directly the phase shift for any given frequency of the induced wave.

Without going into details, which are beyond the scope of this article, we illustrate the photoacoustic effect in Fig. 6, based on a Michelson-type interferometer (25–27). Let us consider an elastic medium with surfaces polished or coated with a reflective tape M [e.g., Mylar (32) tape] in order to increase its reflectivity. A transducer T driving a continuous plane wave produces standing waves at discrete frequencies. A light beam generated by a polarized laser L is launched into a fiber optic system through a beam splitter B. One arm (reference arm) is launched into a fixed-length light guide F. The other (signal) arm is sent to the sensor S, where it is collimated through a cylindrical lens and reflected off the vibrating surface. The reflected back reference and signal arms are then brought to interfere with each other and an intensity-varying

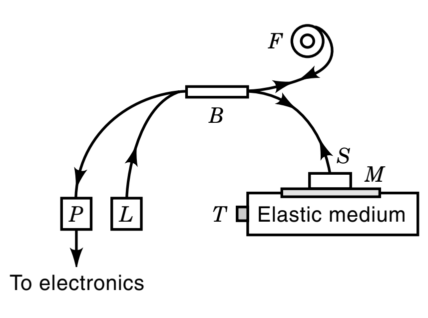

Figure 6. Simple scheme for a fiberoptics sensor.

output signal is created. A photodiode P connected to electronic devices can then measure the changes in light intensity.

If the specimen is enclosed in a rigid tube (e.g., water in a Plexiglas tube; Ref. 33), since the external surface is not sensitive to vibrations, a membrane must be inserted in a hole of the tube in order to sense the pressure variations in the enclosed medium. The standard setup shown in Fig. 6 may be used to implement different techniques by means of fiber optics or laser interferometers. They may achieve a very high sensitivity for displacements, of the order of 1 Å for the Michelson interferometer, and a flat bandwidth response, from 1 kHz to 20 MHz in the case of the Mach-Zender interferometer.

The Mach-Zender interferometer may be either bonded to the surface (29) or embedded in the specimen (30,31). In both cases, the acoustic wave displacement induces a pressure on the light guides (31), leading to axial compression/tension and, therefore, to a phase shift of the propagating light beam. It is sensitive to both in-plane and out-of-plane displacements, but in the case of composites, it has been found to be insensitive to small angular misalignments of fibers with respect to the incoming wave front. The embedded configuration is shown to be several times more sensitive to the wave motion (up to 12 Pa per 1 m length of lightguide in the measuring channel) (e.g., in the case of Lamb waves) than the surface-bonded one. However, the latter configuration may be more practical.

A dual-probe interferometer (34) is based on the interference of two signals received from two fiberoptic receivers located in different positions on the surface of the specimen. A similar approach has been used by Clark, Delsanto, and Mignogna (35,36) using piezoelectric transducers for the determination of times of flight of ultrasonic Rayleigh waves in acoustoelasticity applications (texture and stress measurements in polycrystalline aggregates). However, this technique could be problematic since the signal is affected by the contact transducer it must pass. A different approach, based on the Doppler effect, is at the basis of the Fabry–Perot interferometer (37). If an elastic specimen is subject to vibrations, the reflected light is Doppler shifted and the wavelength shift is related to the surface velocity of the target.

Two major problems lead to signal fading in optical fiber interferometers. The first is represented by a fluctuation in the state of optical polarization within the optical fiber and can be removed by using polarization control or polarization-maintaining fibers. The second concerns changes in the optical phase difference between the interfering channels due, for example, to thermal effects. As a consequence, the device sensitivity can drop to zero when the measurement is performed. To avoid variations in sensitivity, several stabilization schemes have been developed. In the case of homodyne systems, feedback is used in order to lock the interferometer at quadrature; heterodyne techniques allow the environmental noise to be effectively cancelled, but lead to a rise in the demodulation circuitry complexity. Passive stabilization schemes are very efficient but require complex signal processing.

In general, photoacoustic transducers and sensors present several disadvantages compared with piezoelectric transducers. The efficiency of sound generation by thermal sources is rather low and the sensitivity of ultrasonic detection is poorer. However, since these are noncontact devices, they can scan curved surfaces conveniently and measure displacement. Since the optical wavelength is several orders of magnitude smaller than the wavelength of acoustic pulses, the resulting accuracy in the determination of the displacement amplitudes becomes correspondingly better.

SUMMARY

Acoustic interference is due to the superposition of two or more initially coherent sound waves, which are superimposed after they have traveled different acoustic paths. Acoustic interferometry has been used for determining material properties and their dependence on parameters such as temperature or pressure; or the presence of impurities or defects by determining the phase velocity and/or attenuation as a function of these variables. When the geometry of the specimen is properly defined, the phase velocity and attenuation in the specimen can be determined accurately as a function of the physical parameters by using a suitable acoustic interferometer. We have shown various examples of configurations of different interferometers and discussed their usefulness in studying the properties of fluids as well as of solids.

BIBLIOGRAPHY

1. E. P. Papadakis, Ultrasonic velocity and attenuation: Measurement methods with scientific and industrial applications. In W. Mason and R. Thurston (eds.), *Physical Acoustics,* vol. 12, New York: Academic Press, 1976, pp. 277–374.
2. C. M. Fortunko, et al., Absolute measurements of elastic wave phase and group velocities in lossy materials, *Rev. Sci. Instrum.,* **63**: 3477–3486, 1992.
3. Alexander Wood, *Acoustics,* New York: Dover, 1966.
4. T. F. Hueter and R. H. Bolt, *Sonics,* New York: Wiley, 1955.
5. K. W. Katahara, et al., An interferometric technique for measuring velocity and attenuation in molten rocks, *J. Geophys. Res.,* **86**: 11779–11786, 1981.
6. P. M. Nasch, M. H. Manghnani, and R. A. Secco, A modified ultrasonic interferometer for sound velocity measurements in molten metals and alloys, *Rev. Sci. Instrum.,* **65**: 682–688, 1994.
7. M. B. Ewing, M. L. McGlashan, and J. P. M. Trusler, The speed of sound in gases, *J. Chem. Thermodynamics,* **17**: 549–559, 1985.
8. C. H. A. Huan, et al., High-sensitivity ultrasonic interferometer for the detection of magnetic phase transitions, *J. Appl. Phys.,* **61**: 3193–3195, 1987.
9. P. L. M. Heidemann, Determination and correlation of quadrature fringe measurement errors in interferometers, *Appl. Optics,* **20**: 3382–3385, 1981.
10. E. C. Everbach and R. E. Apfel, An interferometric technique for B/A measurement, *J. Acoust. Soc. Amer.,* **98**: 3428–3438, 1995.
11. N. K. Batra and P. P. Delsanto, Ultrasonic interferometric characterization of highly attenuative materials, *J. Acoust. Soc. Amer.,* **85**: 1167–1172, 1989.
12. N. K. Batra, et al., Ultrasonic interferometric characterization of material plates, *Proc. IEEE Ultrason. Symp.,* Cannes, France, pp. 1215–1218, 1994.
13. A. P. Sarvazyan and T. V. Chalikian, Theoretical analysis of an ultrasonic interferometer for precise measurements at high pressures, *Ultrasonics,* **29**: 119–124, 1991.
14. S. P. Klimov, V. V. Tyutekin, and A. E. Vovk, Automated acoustic interferometer, *Meas. Techniques,* **32**: 1198–1201, 1989.
15. V. A. Sukatskas, et al., Density measurement of a liquid with an

ultrasonic interferometer of constant length, *Meas. Techniques,* **31**: 1126–1129, 1988.

16. I. V. Lebedeva and S. P. Dragan, Determination of acoustic characteristics in tubes by means of two microphones, *Meas. Techniques,* **31**: 806–807, 1988.
17. Yu. S. Il'inykh, V. I. Levtsov, and S. S. Sekoyan, Analysis of dynamic characteristics of an ultrasonic interferometer with astatic external control system, *Meas. Techniques,* **31**: 597–601, 1988.
18. L. Cusco and J. P.M. Trusler, Identification of environmentally acceptable low-sound speed liquids, *Int. J. Thermophys.,* **16**: 675–685, 1995.
19. Y. N. Barabenenkov and V. I. Pasechnik, A study of correlations properties of thermal acoustic radiation, *Acoust. Phy.,* **41**: 494–496, 1995.
20. K. H. C. Jhung, et al., Effects of higher-order harmonics on phase determination in an ultrasonic interferometer, *J. Acoust. Soc. Amer.,* **91**: 2025–2029, 1992.
21. A. Migliori and J. L. Sarro, *Resonant Ultrasound Spectroscopy,* New York: Wiley, 1997.
22. A. Briggs, *Acoustic Microscopy,* New York: Oxford University Press, 1992.
23. J. D. Achenbach, J. O. Kim, and Y.-C. Lee, Measuring thin-film elastic constants by line-focus acoustic microscopy, in Andrew Briggs (ed.), *Advances in Acoustic Microscopy,* New York: Academic Press, 1995, Volume 1, pp. 153–208.
24. T. W. Murray, J. B. Deaton, Jr., and J. W. Wagner, Experimental evaluation of enhanced generation of ultrasonic waves using an array of laser sources, *Ultrasonics,* **34**: 69–77, 1996.
25. S. A. Cheyne, C. T. Stebbings, and R. A. Roy, Phase velocity measurements in bubbly liquids using a fiber optic laser interferometer, *J. Acoust. Soc. Amer.,* **97**: 1621–1624, 1995.
26. S. G. Pierce, B. Culshaw, and W. R. Philp, Synchronized triggering for ultrasonic transient detection using optical fiber interferometers and application to the measurement of broadband Lamb wave dispersion characteristics, *Meas. Sci. Technol.,* **7**: 1665–1667, 1996.
27. M. G. Somekh, et al., An accurate noncontacting laser based system for surface wave velocity measurement, *Meas. Sci. Technol.,* **6**: 1329–1337, 1995.
28. S. G. Pierce, et al., Broadband Lamb wave measurements in aluminum and carbon/glass fiber reinforced composite materials using non contacting laser generation and detection, *Ultrasonics,* **35**: 105–114, 1997.
29. S. G. Pierce, et al., Surface-bonded and embedded optical fibers as ultrasonic sensors, *Appl.Opt.,* **35**: 5191–5197, 1996.
30. W. J. Staszewski, et al., Wavelet signal processing for enhanced Lamb wave defect detection in composite plates using optical fiber detection, *Opt. Eng.,* **36**: 1877–1888, 1997.
31. S. X. Short, et al., An experimental study of acoustic vibration effects in optical fibers current sensors, *IEEE Trans. Power Deliv.,* **11**: 1702–1705, 1996.
32. Mylar: Manufactured by DuPont de-Nemours, Barley Mill Plaza, Wilmington, DE, 1980.
33. Plexiglas: Manufactured by AtoHaas Americas Inc., 100-T Independence Mall W., Philadelphia, PA 19105.
34. H. P. Ho, et al., Direct and indirect dual-probe interferometers for accurate surface wave measurements, *Meas. Sci. Technol.,* **5**: 1480–1490, 1994.
35. P. P. Delsanto and A. V. Clark, Jr., Rayleigh wave propagation in deformed orthotropic materials, *J. Acoust. Soc. Amer.,* **81**: 952–960, 1987.
36. P. P. Delsanto, R. B. Mignogna, and A. V. Clark, Jr., Ultrasonic texture and stress measurements in anisotropic polycrystalline aggregates, *J. Acoust. Soc. Amer.,* **87**: 215–224, 1990.
37. D. A. Oursler and J. W. Wagner, Full-field vibrometry using the Fabry-Perot etalon interferometer, *Appl. Opt.,* **31**: 7301–7307, 1992.

N. K. Batra
Naval Research Laboratory
P. P. Delsanto
A. Romano
M. Scalerandi
Politecnico di Torino

ACOUSTOELECTRONIC DEVICES.

See Surface acoustic wave applications.